LMI-BASED TRAJECTORY PLANNING FOR CLOSED-LOOP CONTROL OF ROBOTIC SYSTEMS WITH VISUAL FEEDBACK

Graziano Chesi
Department of Electrical and Electronic Engineering, University of Hong Kong
Pokfulam Road, Hong Kong, China

Keywords: Robot control, Visual feedback, Trajectory planning, LMI.

Abstract: Closed-loop robot control based on visual feedback is an important research area, with useful applications in various fields. Planning the trajectory to be followed by the robot allows one to take into account multiple constraints during the motion, such as limited field of view of the camera and limited workspace of the robot. This paper proposes a strategy for path-planning from an estimate of the point correspondences between the initial view and the desired one, and an estimate of the camera intrinsic parameters. This strategy consists of generating a parametrization of the trajectories connecting the initial location to the desired one via polynomials. The trajectory constraints are then imposed by using suitable relaxations and LMIs (linear matrix inequalities). Some examples illustrate the proposed approach.

1 INTRODUCTION

An important research area in robotics is represented by visual servoing. This area studies the application of closed-loop control in robotic system with visual feedback. Specifically, the problem consists of steering a robot end-effector from an unknown initial location to an unknown desired location by using the visual information provided by a camera. This camera is typically mounted on the robot end-effector, and the configuration is known as eye-in-hand configuration. The camera is firstly located at a certain location, called desired location, and the image projections of some object points visible from this location are recorded. Then, the camera is moved to another location of the robot workspace, from which the same object points are visible, and whose relative motion with respect to the desired location is unknown. The problem, hence, consists of reaching again the desired location from this new location, which is called initial location. See for instance (Hashimoto, 1993; Chaumette and Hutchinson, 2006; Chaumette and Hutchinson, 2007) and references therein.

The procedure just described is known as teaching-by-showing approach. It is well-known that the teaching-by-showing approach has numerous and various applications, for example in the industrial manufacture for the construction of complex components such as parts of a ship, where its function consists of allowing a robotic arm to grasp and position tools and objects. Other applications are in surveillance, where a mobile camera observes some areas of interest such as the entrance of a building in order to identify people, and in airplane alignment, where the system to be positioned is represented by the airplane that has to be aligned with respect to the runway in order to land. Also, the teaching-by-showing approach finds application in surgery, where an instrument is automatically guided to the organ to operate, in navigation, where a mobile robot has to explore a scene, and in dangerous environments such as nuclear stations and spatial missions, where humans should be replaced.

In last years, various methods have been developed for addressing this approach. Some of these methods have proposed the use of the camera pose as feedback information (known as position-based visual servoing, see e.g. (Thuilot et al., 2002)), definition of the feedback error in the image domain (known as image-based visual servoing, see e.g. (Hashimoto et al., 1991)), use of both camera pose error and image error (known as 2 1/2 D visual servoing, see e.g. (Malis et al., 2003)), partition of the degrees of freedoms (Corke and Hutchinson, 2001), switching strategies for ensuring constraints and improving performance (Chesi et al., 2004; Gans and Hutchinson, 2007; Lopez-Nicolas et al., 2007), generation of circular-like trajectories for minimizing the

Chesi G.
LMI-BASED TRAJECTORY PLANNING FOR CLOSED-LOOP CONTROL OF ROBOTIC SYSTEMS WITH VISUAL FEEDBACK.
DOI: 10.5220/0002172200130020
In *Proceedings of the 6th International Conference on Informatics in Control, Automation and Robotics (ICINCO 2009)*, page
ISBN: 978-989-674-000-9

trajectory length (Chesi and Vicino, 2004), control invariant to intrinsic parameters (Malis, 2004), use of complex image features via image moments (Tahri and Chaumette, 2005), global motion plan via navigation functions (Cowan and Chang, 2005), use of cylindrical coordinate systems (Iwatsuki and Okiyama, 2005), enlargement of stability regions (Tarbouriech et al., 2005), and model-less control (Miura et al., 2006).

Path-planning strategies have also been proposed in order to take into account multiple constraints, such as limited field of view of the camera and limited workspace of the robot. See for instance (Mezouar and Chaumette, 2002; Park and Chung, 2003; Deng et al., 2005; Allotta and Fioravanti, 2005; Yao and Gupta, 2007; Kazemi et al., 2009) and references therein. These methods generally adopt potential fields along a reference trajectory in order to fulfill the required constraints, in particular the potential fields do not affect the chosen reference trajectory wherever the constraints are not violated, while they make the camera deviating from this path wherever a constraint does not hold. The planned trajectory is then followed by tracking the image projection of this trajectory through an image-based controller such as the one proposed in (Mezouar and Chaumette, 2002).

In this paper we propose the use of a parametrization of the trajectories connecting the initial location to the desired one, together with the use of dedicated optimization techniques for identifying the trajectories which satisfy the required constraints. Specifically, this parametrization is obtained by estimating the camera pose existing between these two locations and by estimating the position of the object points in the three-dimensional space. These estimations are performed by exploiting the available image point correspondences between the initial and desired views, and by exploiting the available estimate of the camera intrinsic parameters. Then, typical trajectory constraints such as the limited field of view of the camera and the limited workspace of the robot, are formulated in terms of positivity of certain polynomials. The positivity of these polynomials is then imposed by using some suitable relaxations for constrained optimization. These relaxations can be formulated in terms of LMIs (linear matrix inequalities), whose feasibility can be checked via convex programming tools. Some examples are reported to illustrate the application of the proposed approach.

This paper extends our previous works (Chesi and Hung, 2007), where a path-planning method based on the computation of the roots of polynomials was proposed (the advantage with respect to this method is the use of LMIs), and (Chesi, 2009b), where a planning strategy is derived by using homogeneous forms (the advantage with respect to this method is the use of more general relaxations which may allow one to take into account more complex constraints).

The organization of the paper is as follows. Section 2 introduces the notation, problem formulation, and some preliminaries about representation of polynomials. Section 3 describes the proposed strategy for trajectory planning. Section 4 illustrates the simulation and experimental results. Lastly, Section 5 provides some final remarks.

2 PRELIMINARIES

In this section we introduce some preliminaries, namely the notation, problem formulation, and a tool for representing polynomials.

2.1 Notation and Problem Formulation

Let us start by introducing the notation adopted throughout the paper:

- $\mathbb{R}$: real numbers space;
- 0_n: $n \times 1$ null vector;
- I_n: $n \times n$ identity matrix;
- $\|v\|$: euclidean norm of vector v.

We consider a generic stereo vision system, where two cameras are observing a common set of object points in the scene. The symbols F^{ini} and F^{des} represent the frames of the camera in the initial and desired location respectively. These frames are expressed as

$$\begin{array}{rcl} F^{ini} & = & \{R^{ini}, t^{ini}\} \\ F^{des} & = & \{R^{des}, t^{des}\} \end{array} \quad (1)$$

where $R^{ini}, R^{des} \in \mathbb{R}^{3\times 3}$ are rotation matrices, and $t^{ini}, t^{des} \in \mathbb{R}^3$ are translation vectors. These quantities R^{ini}, R^{des}, t^{ini} and t^{des} are expressed with respect to an absolute frame, which is indicated by F^{abs}.

The observed object points project on the image plane of the camera in the initial and desired location onto the image points $p_1^{ini}, \ldots, p_n^{ini} \in \mathbb{R}^3$ (initial view) and $p_1^{des}, \ldots, p_n^{des} \in \mathbb{R}^3$ (desired view). These image points are expressed in homogeneous coordinates according to

$$p_i^{ini} = \begin{pmatrix} p_{i,1}^{ini} \\ p_{i,2}^{ini} \\ 1 \end{pmatrix}, \quad p_i^{des} = \begin{pmatrix} p_{i,1}^{des} \\ p_{i,2}^{des} \\ 1 \end{pmatrix}. \quad (2)$$

where $p_{i,1}^{ini}, p_{i,1}^{des} \in \mathbb{R}$ are the components on the x-axis of the image screen, while $p_{i,2}^{ini}, p_{i,2}^{des} \in \mathbb{R}$ are those on

the y-axis. The projections p_i^{ini} and p_i^{des} are determined by the projective law

$$\begin{array}{rcl} d_i^{ini} p_i^{ini} & = & KR^{ini'}\left(q_i - t^{ini}\right) \\ d_i^{des} p_i^{des} & = & KR^{des'}\left(q_i - t^{des}\right) \end{array} \quad (3)$$

where $d_i^{ini}, d_i^{des} \in \mathbb{R}$ are the depths of the ith point, $q_i \in \mathbb{R}^3$ is the ith point expressed with respect to F^{abs}, and $K \in \mathbb{R}^{3\times 3}$ is the upper triangular matrix containing the intrinsic parameters of the camera.

The problem we consider in this paper consists of planning a trajectory from the initial location F^{ini} to the desired one F^{des} (which are unknown) by using the available estimates of:

1. the image projections $\hat{p}_1^{ini}, \hat{p}_1^{des}, \ldots, \hat{p}_n^{ini}, \hat{p}_n^{des}$;
2. and intrinsic parameters matrix $\hat{K}$.

This trajectory must ensure that the object points are kept inside the field of view of the camera, and that the camera does not exit its allowed workspace.

In the sequel, we will indicate the set of rotation matrices in $\mathbb{R}^{3\times 3}$ as $SO(3)$, and the set of frames in the three-dimensional space as $SE(3)$, where $SE(3) = SO(3) \times \mathbb{R}^3$.

2.2 Representation of Polynomials

Before proceeding, let us briefly introduced a tool for representing polynomials which will be exploited in the sequel. Let $p(x)$ be a polynomial of degree $2m$ in the variable $x = (x_1, \ldots, x_n)' \in \mathbb{R}^n$, i.e.

$$p(x) = \sum_{\substack{i_1 + \ldots + i_n \le 2m \\ i_1 \ge 0, \ldots, i_n \ge 0}} c_{i_1,\ldots,i_n} x_1^{i_1} \cdots x_n^{i_n} \quad (4)$$

for some coefficients $c_{i_1,\ldots,i_n} \in \mathbb{R}$. Then, $p(x)$ can be expressed as

$$p(x) = x^{\{m\}'} P(\alpha) x^{\{m\}} \quad (5)$$

where $x^{\{m\}}$ is any vector containing a base for the polynomials of degree m in x, and hence can be simply chosen as the set of monomials of degree less than or equal to m in x, for example via

$$x^{\{m\}} = (1, x_1, \ldots, x_n, x_1^2, x_1 x_2, \ldots, x_n^m)', \quad (6)$$

and

$$P(\alpha) = P + L(\alpha) \quad (7)$$

where $P = P'$ is a symmetric matrix such that

$$p(x) = x^{\{m\}'} P x^{\{m\}}, \quad (8)$$

while $L(\alpha)$ is a linear parametrization of the linear space

$$\mathcal{L}(n,m) = \{L = L' : \; x^{\{m\}'} L x^{\{m\}} = 0 \;\; \forall x\} \quad (9)$$

being α a vector of free parameters. The dimension of $x^{\{m\}}$ is given by

$$\sigma(n,m) = \frac{(n+m)!}{n!m!} \quad (10)$$

while the dimension of α (i.e., the dimension of $\mathcal{L}$) is

$$\tau(n,m) = \frac{1}{2}\sigma(n,m)(\sigma(n,m)+1) - \sigma(n,2m). \quad (11)$$

The representation in (5) was introduced in (Chesi et al., 1999) with the name SMR (square matricial representation). The matrices P and $P(\alpha)$ are known as SMR matrices of $p(x)$, and can be computed via simple algorithms. See also (Chesi et al., 2003; Chesi et al., 2009).

The SMR was introduced in (Chesi et al., 1999) in order to investigate positivity of polynomials via convex optimizations. Indeed, $p(x)$ is clearly positive if it is a sum of squares of polynomials, and this latter condition holds if and only if there exists α such that

$$P(\alpha) \ge 0 \quad (12)$$

which is an LMI (linear matrix inequality). It turns out that, establishing whether an LMI admits a feasible solution or not, amounts to solving a convex optimization.

3 TRAJECTORY PLANNING

This section describes the proposed approach. Specifically, we first introduce the adopted parametrization of the trajectories, then we describe the computation of the trajectory satisfying the required constraints, and lastly we explain how the camera pose and object points can be estimated from the available data.

3.1 Trajectory Parametrization

Let us start by parameterizing the trajectory of the camera from the initial location to the desired one. This can be done by denoting the frame of the camera along the trajectory as

$$F(a) = \{R(a), t(a)\} \quad (13)$$

where $a \in [0,1]$ is the normalized trajectory abscise, $R(a) \in SO(3)$ is the rotation matrix of $F(a)$, and $t(a) \in \mathbb{R}^3$ is the translation vector. We choose the convention

$$\begin{array}{rcl} a = 0 & \rightarrow & F(a) = F^{ini} \\ a = 1 & \rightarrow & F(a) = F^{des}. \end{array} \quad (14)$$

The functions $R : [0,1] \rightarrow SO(3)$ and $t : [0,1] \rightarrow \mathbb{R}^3$ must satisfy the boundary conditions

$$\begin{array}{rclrcl} R(0) & = & \hat{R}^{ini}, & R(1) & = & \hat{R}^{des} \\ t(0) & = & \hat{t}^{ini}, & t(1) & = & \hat{t}^{des} \end{array} \quad (15)$$

where $\hat{R}^{ini}$, $\hat{R}^{des}$, $\hat{t}^{ini}$ and $\hat{t}^{des}$ are the available estimates of R^{ini}, R^{des}, t^{ini} and t^{des} (the computation of these estimates will be addressed in Section 3.3). We adopt polynomials in order to parameterize $R(a)$ and $t(a)$. Specifically, we parameterize $t(a)$ according to

$$t(a) = \sum_{i=0}^{\delta} \check{t}_i a^i \tag{16}$$

where δ is an integer representing the chosen degree for $t(a)$, and $\check{t}_0, \ldots, \check{t}_\delta \in \mathbb{R}^3$ are vectors to be determined. Then, we parameterize $R(a)$ as

$$R(a) = \frac{E(r(a))}{\|r(a)\|^2} \tag{17}$$

where $E : \mathbb{R}^4 \to SO(3)$ is the parametrization of a rotation matrix via Euler parameters, which is given by

$$E(r) = \begin{pmatrix} r_1^2 - r_2^2 - r_3^2 + r_4^2 & 2(r_1 r_2 - r_3 r_4) & 2(r_1 r_3 + r_2 r_4) \\ 2(r_1 r_2 + r_3 r_4) & -r_1^2 + r_2^2 - r_3^2 + r_4^2 & 2(r_2 r_3 - r_1 r_4) \\ 2(r_1 r_3 - r_2 r_4) & 2(r_2 r_3 + r_1 r_4) & -r_1^2 - r_2^2 + r_3^2 + r_4^2 \end{pmatrix} \tag{18}$$

while $r : [0,1] \in \mathbb{R}^4$ denotes the Euler parameter along the trajectory. It turns out that

$$E(r) \in SO(3) \;\; \forall r \in \mathbb{R}^4 \setminus \{0_4\}, \tag{19}$$

and moreover

$$\forall R \in SO(3) \; \exists \xi(R) \in \mathbb{R}^4 \setminus \{0_4\} : \; E(\xi(R)) = R, \tag{20}$$

in particular

$$\xi(R) = \begin{pmatrix} \sin\frac{\theta}{2} u \\ \cos\frac{\theta}{2} \end{pmatrix} \tag{21}$$

where $\theta \in [0, \pi]$ and $u \in \mathbb{R}^3$, $\|u\| = 1$, are respectively the rotation angle and axis in the exponential coordinates of R, i.e.

$$R = e^{[\theta u]_\times}. \tag{22}$$

We parameterize $r(a)$ according to

$$r(a) = \sum_{i=0}^{\gamma} \check{r}_i a^i \tag{23}$$

where $\check{r}_0, \ldots, \check{r}_\gamma \in \mathbb{R}^4$ are vectors for some integer γ. The boundary conditions in (15) become, hence,

$$\begin{array}{rclcrcl} \check{r}_0 & = & \xi(\hat{R}^{ini}), & & \sum_{i=0}^{\gamma} \check{r}_i & = & \xi(\hat{R}^{des}) \\ \check{t}_0 & = & \hat{t}^{ini}, & & \sum_{i=0}^{\delta} \check{t}_i & = & \hat{t}^{des} \end{array} \tag{24}$$

which imply that $r(a)$ and $t(a)$ can be re-parameterized as

$$\begin{array}{rcl} r(a) & = & \left(\xi(\hat{R}^{des}) - \xi(\hat{R}^{ini}) - \sum_{i=1}^{\gamma-1} \bar{r}_i\right) a^\gamma \\ & & + \sum_{i=1}^{\gamma-1} \bar{r}_i a^i + \xi(\hat{R}^{ini}) \\ t(a) & = & \left(\hat{t}^{des} - \hat{t}^{ini} - \sum_{i=1}^{\delta-1} \bar{t}_i\right) a^\delta + \sum_{i=1}^{\delta-1} \bar{t}_i a^i + \hat{t}^{ini} \end{array} \tag{25}$$

where $\bar{r}_1, \ldots, \bar{r}_{\gamma-1} \in \mathbb{R}^4$ and $\bar{t}_1, \ldots, \bar{t}_{\delta-1} \in \mathbb{R}^3$ are free vectors.

Let us observe that the derived parametrization can describe arbitrarily complicated trajectories, simply by selecting sufficiently large degrees γ and δ. Moreover, it is useful to observe that special cases such as straight lines are simply recovered by the choices

$$\begin{array}{c} \gamma = 1 \text{ (straight line in the domain of } E) \\ \delta = 1 \text{ (straight line in the translational space).} \end{array} \tag{26}$$

For ease of description we will assume $\gamma = 1$ in the following sections.

3.2 Trajectory Computation

In this section we address the problem of identifying which trajectories inside the introduced parametrization satisfy the required trajectory constraints. Due to space limitation, we describe only two fundamental constraints, in particular the visibility constraint (the object points must remain in the field of view of the camera) and the workspace constraint (the camera cannot exit from its allowed workspace). Other constraints can be similarly considered.

Let us indicate with $p_i(a) = (p_{i,1}(a), p_{i,2}(a), 1)' \in \mathbb{R}^3$ the image projection of the ith object point along the trajectory. The visibility constraint is fulfilled whenever

$$p_{i,j}(a) \in (s_{i,1}, s_{i,2}) \;\; \forall i = 1, \ldots, n \; \forall j = 1,2 \; \forall a \in [0,1] \tag{27}$$

where $s_{1,1}, s_{1,2}, s_{2,1}, s_{2,2} \in \mathbb{R}$ are the screen limits. We estimate $p_i(a)$ via

$$\begin{array}{rcl} p_i(a) & = & \dfrac{f_i(a)}{f_{i,3}(a)} + (1-a)\left(\hat{p}_i^{ini} - \dfrac{f_i(0)}{f_{i,3}(0)}\right) \\ & & + a\left(\hat{p}_i^{des} - \dfrac{f_i(1)}{f_{i,3}(1)}\right) \end{array} \tag{28}$$

where $f_i(a) = (f_{i,1}(a), f_{i,2}(a), f_{i,3}(a))' \in \mathbb{R}^3$ is

$$f_i(a) = \hat{K} E(r(a))' (\hat{q}_i - t(a)) \tag{29}$$

and $\hat{q}_i \in \mathbb{R}^3$ is the estimate of the object point q_i (the computation of this estimate will be addressed in Section 3.3). Let us observe that this choice ensures

$p_i(0) = \hat{p}_i^{ini}$ and $p_i(1) = \hat{p}_i^{des}$. We can rewrite $p_i(a)$ as

$$p_i(a) = \frac{1}{f_{i,3}(a)} \begin{pmatrix} g_{i,1}(a) \\ g_{i,2}(a) \\ f_{i,3}(a) \end{pmatrix} \tag{30}$$

where $g_{i,1}(a), g_{i,2}(a) \in \mathbb{R}$ are polynomials.

Then, let us consider the workspace constraint. A possible way to define the workspace constraint is via inequalities such as

$$d_i'(t(a_i) - o_i) > w_i \;\; \forall i = 1, \ldots, n_w \tag{31}$$

where $d_i \in \mathbb{R}^3$ is the direction along which the constraint is imposed, $a_i \in [0,1]$ specifies where the constraint is imposed on the trajectory, $o_i \in \mathbb{R}^3$ locates the constraint, $w_i \in \mathbb{R}$ specifies the minimum distance allowed from the point o_i along the direction d_i, and n_w is the number of constraints.

Hence, let us define the set of polynomials

$$\begin{aligned} \mathcal{H} \;=\; & \{ s_{j,k} f_{i,3}(a) - (-1)^k g_{i,j}(a) \; \forall i = 1, \ldots, n, \\ & j,k = 1,2 \} \;\cup\; \{ f_{i,3}(a) \; \forall i = 1, \ldots, n \} \\ & \cup \{ d_i'(t(a_i) - o_i) - w_i \; \forall i = 1, \ldots, n_w \}. \end{aligned} \tag{32}$$

The visibility and workspace constraints are hence fulfilled whenever

$$h(a) > 0 \;\; \forall h(a) \in \mathcal{H} \;\; \forall a \in [0,1]. \tag{33}$$

For each polynomial $h(a)$ in $\mathcal{H}$, let us introduce an auxiliary polynomial $u_h(a)$ of some degree, and let us define

$$v_h(a) = h(a) - a(1-a)u_h(a). \tag{34}$$

Let us express these polynomials via the SMR as

$$\begin{array}{rcl} u_h(a) & = & y_h(a)' U_h y_h(a) \\ v_h(a) & = & z_h(a)' V_h(\alpha_h) z_h(a) \end{array} \tag{35}$$

where $y_h(a), z_h(a)$ are vectors containing polynomial bases, and $U, V(\alpha_h)$ are symmetric SMR matrices (see Section 2.2 for details). It can be verified that (33) holds whenever the following set of LMIs is satisfied:

$$\left.\begin{array}{rcl} U_h & > & 0 \\ V_h(\alpha_h) & > & 0 \end{array}\right\} \;\; \forall h(a) \in \mathcal{H}. \tag{36}$$

The LMI feasibility test (36) provides a sufficient condition for the existence of a trajectory satisfying the required constraints. Hence, it can happen that this condition is not satisfied even if a trajectory does exist. However, it should be observed that the conservatism of this condition decreases by increasing the degree of the polynomials used to parameterize the trajectory.

3.3 Camera Pose and Scene Estimation

In the previous sections we have described how the trajectory of the camera can be parameterized and computed. In particular, the parametrization was based on the estimates $\hat{R}^{ini}$, $\hat{R}^{des}$, $\hat{t}^{ini}$ and $\hat{t}^{des}$ of the components of the initial and desired frames F^{ini} and F^{des}, while the computation was based on the estimates $\hat{q}_1, \ldots, \hat{q}_n$ of the object points $q_1, \ldots, q_n$. Here we describe some ways to obtain these estimates.

Given the estimates $\hat{p}_1^{ini}, \hat{p}_1^{des}, \ldots, \hat{p}_n^{ini}, \hat{p}_n^{des}$ of the image projections and $\hat{K}$ of the intrinsic parameters matrix, one can estimate the camera pose between F^{ini} and F^{des}, and hence R^{ini} and t^{ini} since F^{des} can be chosen without loss of generality equal to F^{abs}. This estimation can be done, for example, through the essential matrix or through the homography matrix, see for instance (Malis and Chaumette, 2000; Chesi and Hashimoto, 2004; Chesi, 2009a) and references therein.

Once that the estimates $\hat{R}^{ini}$ and $\hat{t}^{ini}$ have been found, one can compute the estimates $\hat{q}_1, \ldots, \hat{q}_n$ of the object points via a standard triangulation scheme, which amounts to solving a linear least-squares problem.

Let us observe that, if no additional information is available, the translation vector and the object points can be estimated only up to a scale factor. In this case, the workspace constraint has to be imposed in a normalized space. This problem does not exist if a CAD model of the object (or part of it) is available, since this allows to estimate the distance between the origins of F^{ini} and F^{des}.

4 ILLUSTRATIVE EXAMPLES

In this section we present some illustrative examples of the proposed approach. Let us consider the situation shown in Figure 1a, where a camera observes some object points (the centers of the nine large dots in the “2”, “3” and ”4” faces of the three dices) from the initial and desired locations (leftmost and rightmost cameras respectively). Figure 1b shows the image projections of these points in the initial view (“o” marks) and desired view (“x” marks). The intrinsic parameters matrix is chosen as

$$K = \begin{pmatrix} 400 & 0 & 320 \\ 0 & 300 & 240 \\ 0 & 0 & 1 \end{pmatrix}. \tag{37}$$

The problem consists of planning a trajectory from the initial location to the desired one which ensures that the object points are kept inside the field of view

of the camera and the camera does not collide with the sphere interposed between F^{ini} and F^{des} (which represents an obstacle to avoid).

Let us use the proposed approach. We parameterize the trajectory as described in Section 3.1 with polynomials of degree two by estimating the camera pose between F^{ini} and F^{des} via the essential matrix. Then, we build the set of polynomials $\mathcal{H}$, which impose the visibility and workspace constraints. The workspace constraint is chosen by requiring that the trajectory must remain at a certain distance from the obstacle in two directions. Hence, we compute the SMR matrices U_h and $V_h(\alpha_h)$ in (35), and by using the LMI toolbox of Matlab we find that the LMIs in (36) are feasible, in particular the obtained feasible trajectory is shown in Figures 1a and 1b.

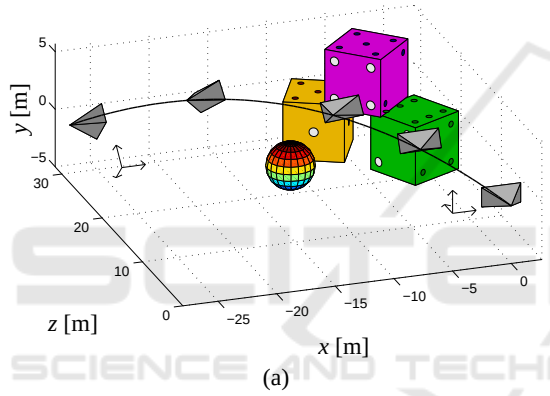

(a)

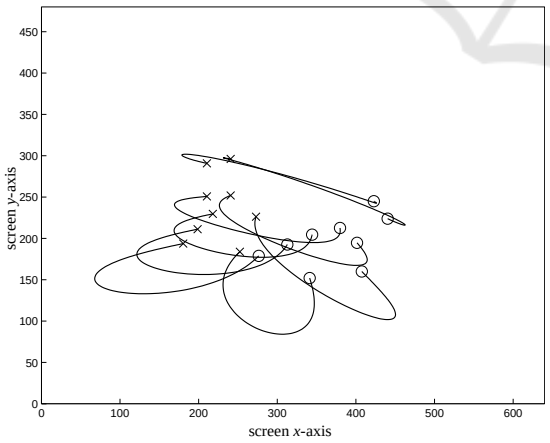

(b)

Figure 1: (a) Initial frame F^{ini} (leftmost camera), desire frame F^{des} (rightmost camera), object points (centers of the nine large dots in the “2”, “3” and ”4” faces of the three dices), planned trajectory (solid line), and some intermediate locations of the camera along the planned trajectory. (b) Image projections of the object points in the initial view (“o” marks) and desired view (“x” marks), and image projection of the planned trajectory (solid line).

Now, in order to introduce typical uncertainties of real experiments, we corrupt the image projections of the object points by adding image noise with uniform distribution in $[-1,1]$ pixels to each component. Moreover, we suppose that the camera is coarsely calibrated, in particular the available estimate of the intrinsic parameters matrix is

$$\hat{K} = \begin{pmatrix} 430 & 0 & 338 \\ 0 & 275 & 250 \\ 0 & 0 & 1 \end{pmatrix}. \qquad (38)$$

We repeat the previous steps in the presence of these uncertainties, and then we track the planned trajectory by using the image-based controller proposed in (Mezouar and Chaumette, 2002). Figures 2a and 2b show the obtained results: as we can see, the camera reaches the desired location by avoiding collisions with the obstacle in spite of the introduced uncertainties.

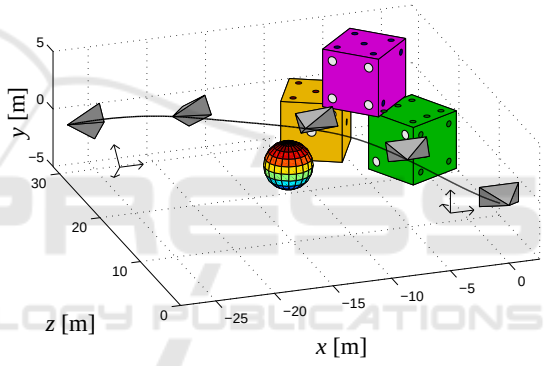

(a)

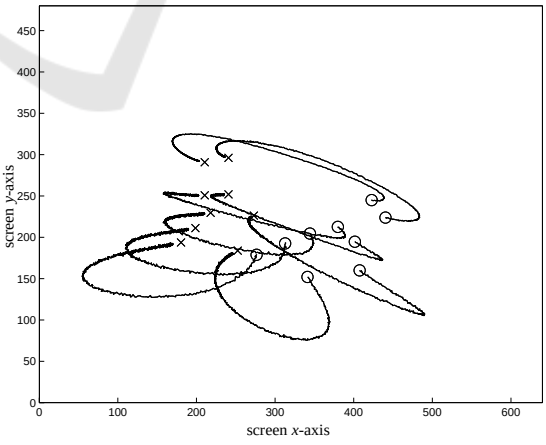

(b)

Figure 2: Results obtained by planning the trajectory with image noise and calibration errors, and by tracking the planned trajectory with an image-based controller.

Lastly, we consider a more difficult case by introducing three obstacles as shown in Figure 3a. We

find that the LMIs are feasible by using polynomials of degree three, and the found solution provides the trajectory shown in Figures 3a and 3b, which satisfies the required constraints.

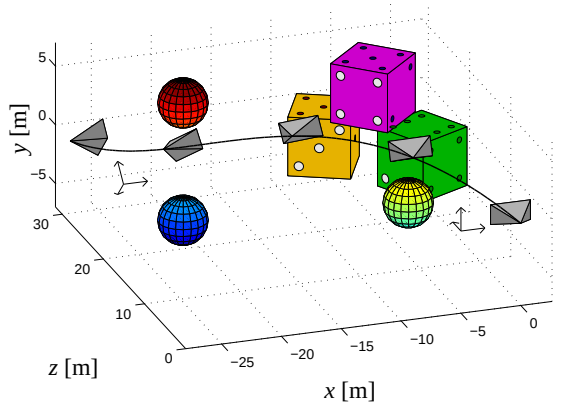

(a)

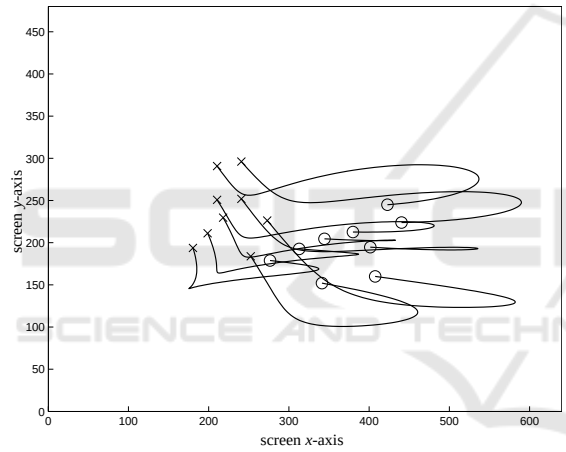

(b)

Figure 3: Results obtained for a different set of obstacles.

5 CONCLUSIONS

We have proposed a trajectory planning strategy for closed-loop control of robotic systems with visual feedback, which allows one to take into account multiple constraints during the motion such as limited field of view of the camera and limited workspace of the robot. This strategy is based on generating a parametrization of the trajectories connecting the initial location to the desired one. The trajectory constraints are imposed by using polynomial relaxations and LMIs. Future work will investigate the application of the proposed approach in real experiments.

ACKNOWLEDGEMENTS

The author would like to thank the Reviewers for their time and useful comments. This work was supported by the Research Grants Council of Hong Kong Special Administrative Region under Grant HKU711208E.

REFERENCES

Allotta, B. and Fioravanti, D. (2005). 3D motion planning for image-based visual servoing tasks. In *Proc. IEEE Int. Conf. on Robotics and Automation*, Barcelona, Spain.

Chaumette, F. and Hutchinson, S. (2006). Visual servo control, part I: Basic approaches. *IEEE Robotics and Automation Magazine*, 13(4):82–90.

Chaumette, F. and Hutchinson, S. (2007). Visual servo control, part II: Advanced approaches. *IEEE Robotics and Automation Magazine*, 14(1):109–118.

Chesi, G. (2009a). Camera displacement via constrained minimization of the algebraic error. *IEEE Trans. on Pattern Analysis and Machine Intelligence*, 31(2):370–375.

Chesi, G. (2009b). Visual servoing path-planning via homogeneous forms and LMI optimizations. *IEEE Trans. on Robotics*, 25(2):281–291.

Chesi, G., Garulli, A., Tesi, A., and Vicino, A. (2003). Solving quadratic distance problems: an LMI-based approach. *IEEE Trans. on Automatic Control*, 48(2):200–212.

Chesi, G., Garulli, A., Tesi, A., and Vicino, A. (2009). *Homogeneous Polynomial Forms for Robustness Analysis of Uncertain Systems*. Springer (in press).

Chesi, G. and Hashimoto, K. (2004). A simple technique for improving camera displacement estimation in eye-in-hand visual servoing. *IEEE Trans. on Pattern Analysis and Machine Intelligence*, 26(9):1239–1242.

Chesi, G., Hashimoto, K., Prattichizzo, D., and Vicino, A. (2004). Keeping features in the field of view in eye-in-hand visual servoing: a switching approach. *IEEE Trans. on Robotics*, 20(5):908–913.

Chesi, G. and Hung, Y. S. (2007). Global path-planning for constrained and optimal visual servoing. *IEEE Trans. on Robotics*, 23(5):1050–1060.

Chesi, G., Tesi, A., Vicino, A., and Genesio, R. (1999). On convexification of some minimum distance problems. In *5th European Control Conf.*, Karlsruhe, Germany.

Chesi, G. and Vicino, A. (2004). Visual servoing for large camera displacements. *IEEE Trans. on Robotics*, 20(4):724–735.

Corke, P. I. and Hutchinson, S. (2001). A new partitioned approach to image-based visual servo control. *IEEE Trans. on Robotics and Automation*, 17(4):507–515.

Cowan, N. J. and Chang, D. E. (2005). Geometric visual servoing. *IEEE Trans. on Robotics*, 21(6):1128–1138.

Deng, L., Janabi-Sharifi, F., and Wilson, W. J. (2005). Hybrid motion control and planning strategy for visual servoing. *IEEE Trans. on Industrial Electronics*, 52(4):1024–1040.

Gans, N. and Hutchinson, S. (2007). Stable visual servoing through hybrid switched-system control. *IEEE Trans. on Robotics*, 23(3):530–540.

Hashimoto, K. (1993). *Visual Servoing: Real-Time Control of Robot Manipulators Based on Visual Sensory Feedback*. World Scientific, Singapore.

Hashimoto, K., Kimoto, T., Ebine, T., and Kimura, H. (1991). Manipulator control with image-based visual servo. In *Proc. IEEE Int. Conf. on Robotics and Automation*, pages 2267–2272.

Iwatsuki, M. and Okiyama, N. (2005). A new formulation of visual servoing based on cylindrical coordinate system. *IEEE Trans. on Robotics*, 21(2):266–273.

Kazemi, M., Gupta, K., and Mehran, M. (2009). Global path planning for robust visual servoing in complex environments. In *Proc. IEEE Int. Conf. on Robotics and Automation*, Kobe, Japan.

Lopez-Nicolas, G., Bhattacharya, S., Guerrero, J. J., Sagues, C., and Hutchinson, S. (2007). Switched homography-based visual control of differential drive vehicles with field-of-view constraints. In *Proc. IEEE Int. Conf. on Robotics and Automation*, pages 4238–4244, Rome, Italy.

Malis, E. (2004). Visual servoing invariant to changes in camera-intrinsic parameters. *IEEE Trans. on Robotics and Automation*, 20(1):72–81.

Malis, E. and Chaumette, F. (2000). 2 1/2 D visual servoing with respect to unknown objects through a new estimation scheme of camera displacement. *Int. Journal of Computer Vision*, 37(1):79–97.

Malis, E., Chesi, G., and Cipolla, R. (2003). 2 1/2 D visual servoing with respect to planar contours having complex and unknown shapes. *Int. Journal of Robotics Research*, 22(10):841–853.

Mezouar, Y. and Chaumette, F. (2002). Path planning for robust image-based control. *IEEE Trans. on Robotics and Automation*, 18(4):534–549.

Miura, K., Hashimoto, K., Inooka, H., Gangloff, J. A., and de Mathelin, M. F. (2006). Model-less visual servoing using modified simplex optimization. *Journal Artificial Life and Robotics*, 10(2):131–135.

Park, J. and Chung, M. (2003). Path planning with uncalibrated stereo rig for image-based visual servoing under large pose discrepancy. *IEEE Trans. on Robotics and Automation*, 19(2):250–258.

Tahri, O. and Chaumette, F. (2005). Point-based and region-based image moments for visual servoing of planar objects. *IEEE Trans. on Robotics*, 21(6):1116–1127.

Tarbouriech, S., Soueres, P., and Gao, B. (2005). A multicriteria image-based controller based on a mixed polytopic and norm-bounded representation of uncertainties. In *44th IEEE Conf. on Decision and Control and European Control Conf.*, pages 5385–5390, Seville, Spain.

Thuilot, B., Martinet, P., Cordesses, L., and Gallice, J. (2002). Position based visual servoing: keeping the object in the field of vision. In *Proc. IEEE Int. Conf. on Robotics and Automation*, pages 1624–1629, Washington, D.C.

Yao, Z. and Gupta, K. (2007). Path planning with general end-effector constraints. *Robotics and Autonomous Systems*, 55(4):316–327.